

# Spike generation governed by the stochasticion adsorption-desorption process

Hirohisa Tamagawa (✉ [tmgwhrhs@gifu-u.ac.jp](mailto:tmgwhrhs@gifu-u.ac.jp))

Gifu University

Kota Ikeda

Meiji (Japan)

Bernard Delalande

Freelance

Titus Mulembo

Dedan Kimathi University of Technology

---

## Research Article

**Keywords:** membrane potential, action potential, mass action law, thermodynamics, stochastic process

**Posted Date:** August 29th, 2022

**DOI:** <https://doi.org/10.21203/rs.3.rs-1994870/v1>

**License:** © ⓘ This work is licensed under a Creative Commons Attribution 4.0 International License.

[Read Full License](#)

---

# Spike generation governed by the stochastic ion adsorption-desorption process

Hirohisa Tamagawa<sup>1\*</sup>, Kota Ikeda<sup>2</sup>, Bernard Delalande<sup>3</sup>  
and Titus Mulembo<sup>4</sup>

<sup>1\*</sup>Department of Mechanical Engineering, Faculty of Engineering,  
Gifu University, 1-1 Yanagido, Gifu, Gifu, 501-1193, Japan.

<sup>2</sup>School of Interdisciplinary Mathematical Sciences, Meiji  
University, 4-21-2, Nakano, Nakano, Tokyo, 164-8525, Japan.

<sup>3</sup>280 avenue de la Pierre Dourant, 38290, La Verpilliere, France.

<sup>4</sup>Mechatronic Engineering department, Dedan Kimathi  
University of Technology DEKUT, Nyeri, Kenya.

\*Corresponding author(s). E-mail(s): [tmgwhrhs@gifu-u.ac.jp](mailto:tmgwhrhs@gifu-u.ac.jp);

Contributing authors: [ikeda@meiji.ac.jp](mailto:ikeda@meiji.ac.jp);

[bernard@somasimple.com](mailto:bernard@somasimple.com); [titusmulembo@gmail.com](mailto:titusmulembo@gmail.com);

## Abstract

There is a deep conviction that the generation of the action potential is one of the most fundamental biological activities. According to the membrane theory, active ion transport and its flow variations across the plasma membrane are responsible for generating the action potential. However, in contrast to the living model, an in vitro model based on the adsorption-desorption process of ions could equally well explain the generation of the action potential. The authors constructed such a model and mathematically related it using the stochastic differential equation (SDE). This SDE model is consistent with the kinetics of the reaction and explains the generation of the action potential. Therefore, it is physiologically important to re-examine the mechanism of action potential generation from the perspective of the ion adsorption-desorption model.

**Keywords:** membrane potential, action potential, mass action law, thermodynamics, stochastic process

# 1 Introduction

An elucidation of the generation mechanism of action potential was a physiologically attractive and important research topic last century. At present, all physiology textbooks refer to the membrane theory to explain the mechanism of action potential generation [1–5]. It states that the change in the rate of ion flow across the plasma membrane is responsible for generating the action potential. Therefore, researchers agree that the generation of the action potential is fully explained by the membrane theory. Several decades ago, researchers believed that they had already identified the functional proteins that regulate transmembrane ion flow. These proteins are called ion channels and ion pumps. In particular, the operation of the pump is seen as an indication of life since it consumes ATP energy. Thus, the generation of the action potential would inevitably be accompanied by a basal metabolic rate. However, some research groups have objected to such a conventional view of the principle of action potential generation. A leader of these researchers is Gilbert Ling [4–6]. Ling presented his physiological theory called the association-induction hypothesis (AIH). In short, the AIH attributes the generation of the action potential to the process of adsorption-desorption of ions. Therefore, the phenomenon of action potential generation is not limited to living systems but can also occur in non-living systems. Fox et al. observed a spontaneous electrical signal with artificially created microspheres.[7–14]. In particular, the electrical signal of the ref.[13, 14] seems indistinguishable from the action potential of a real living cell. It is therefore only natural to ask certain questions: "Is the action potential caused by transmembrane ion flow?" and "Is the action potential a consequence of vital activity?" Fox's microspheres are mainly composed of amino acids. It can therefore still be argued that the microsphere is artificially created but is composed of biological substances. Therefore, some might say

that the generation of an action potential is still an indication of life. But in the field of nonlinear dynamics research, the generation of action potentials of non-living systems in aqueous solution is well known and has been studied intensively. Yoshikawa's works are typical ones [15–22]. They made measurements of the potential generated across the different artificial separators (a sort of membrane) separating two different electrolyte solutions. They observed a frequent generation of potential peaks. Similar studies have been carried out several times to date by other research groups [23–28]. As another type of artificial system, it has been known that corrosion causes a regular potential spike generation [29–31]. Thus, the generation of potential peaks in the aqueous system is a quite ordinary and common natural phenomenon in non-physiological fields of science, it does not seem to require a sophisticated system.

In this paper, the generation of peak potentials observed in the metal-aqueous solution system, which is an inanimate system, is first shown. Then, the observed peak potential will be formulated using the stochastic model. Finally, the mechanism of action potential generation is discussed.

## 2 Experimental observation

First, we performed the following experiments. A metal wire was immersed in an aqueous solution of KCl and its surface potential was measured as a function of time using the set-up shown in Fig.1.

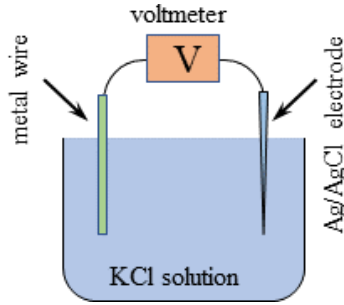


**Fig. 1:** Experimental setup for measuring the wire surface potential. A metal wire is submerged in a KCl aqueous solution.

Two types of metal wire, a nickel wire and a gold wire, were used, and Fig. 2 shows the experimentally measured surface potential profiles. The nickel wire surface showed continuous potential peaks, while the gold wire surface did not. These potential characteristics are mathematically theorised step by step in the following sections.

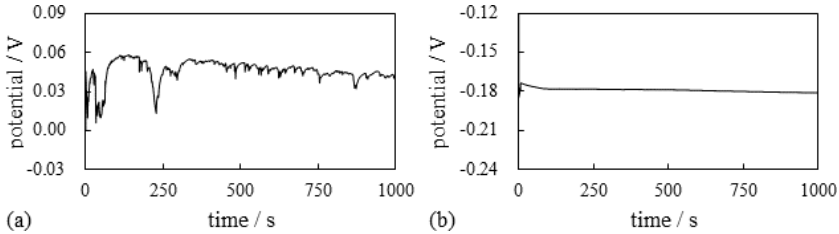


**Fig. 2:** Experimental surface potential of a wire submerged in a  $10^{-4}$ M KCl aqueous solution. The wire used was (a) a nickel wire and (b) a gold wire.

### 3 Potential generation

Previous work suggests that the potential characteristics are governed by the adsorption of ions on the wire surface [32, 33]. In other words, the mobile ions  $i$  adsorb onto the  $s$  ion adsorption sites of the metal surface, as illustrated in Fig. 3. As the ion carries a non-zero charge, the association-dissociation between  $i$  and  $s$  results in the generation of a non-zero surface potential and

its variation. This is the mechanism of membrane potential generation based on ion adsorption.

Let us see the process of generating potential peaks based on the adsorption-desorption mechanism of ions. The non-zero surface potential of the wire when in contact with the demineralised water was observed experimentally (there are no mobile  $i$  ions). Therefore, to treat these experimental systems mathematically, we hypothesised that the hypothetical charges were created on the surface of the wire when it was in an aqueous solution. We introduce  $\rho$  which represents the density of the hypothetical surface charge formed on the surface of the wire when it is immersed in deionised water.

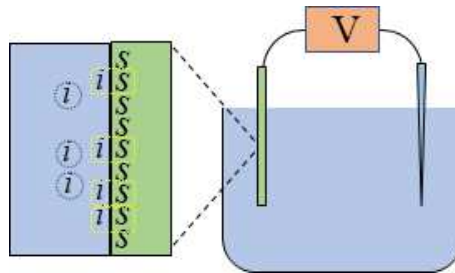


**Fig. 3:** Association and dissociation between the metal wire surface site  $s$  and mobile ion  $i$  in the electrolytic solution.  $i$  encircled by the dotted line represents the free  $i$  in the vicinity of the metal surface.  $is$  encircled by the dashed line represents the  $is$  created by the binding between  $i$  and  $s$ .

According to electromagnetism, it is easy to imagine that the charge separation between  $i$  and  $s$  generates a non-zero potential and that the combination of  $i$  and  $s$  more or less neutralises their charges, causing the potential to change. If the ion adsorption-desorption process shown in Fig. 4 occurs endlessly, the potential spike could be generated repeatedly.

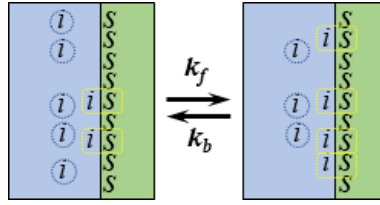


**Fig. 4:** Adsorption-desorption process between  $i$  and  $s$

We have assumed that the adsorption site  $s$  carries the opposite charge to that of the free ion  $i$ . Therefore, the adsorption of an  $i$  on an  $s$  results in the creation of an  $is$  which carries the zero charge. In other words, the charge on  $s$  is neutralised by the charge on  $i$  due to the creation of  $is$ . Assuming further that the adsorption site of a single  $s$  ion carries a charge whose absolute value is  $|e|$  ( $e$ : elementary charge), the number site density of the total adsorption site,  $S_T$ , can be given by Eq.1.

$$S_T = \frac{|\rho|}{|e|} \quad (1)$$

We introduce here  $S_s$  and  $S_{is}$  which represent the number densities of the unoccupied adsorption site  $s$  and the occupied site  $s$  (i.e.  $is$ ), respectively.  $S_s$  and  $S_{is}$  suffice Eq.2. In summary, an occupied  $s$  (i.e.  $is$ ) carries a zero charge, while an unoccupied  $s$  carries a non-zero charge. Thus,  $S_s$  (or  $S_T - S_{is}$ ) governs the characteristics of the metal surface potential.

$$S_T = S_s + S_{is} \quad (2)$$

## 4 Mathematical formula

Based on the concept introduced in the previous section, we have mathematically theorised the potential spike generation mechanism as follows.

Assuming that the ion adsorption-desorption phenomenon on the metal wire surface is a stochastic process, a formula representing the quantity of  $s$  is derived. The association and dissociation between  $s$  and  $i$  is given by Eq.3. Hence, Eq.4 is derived from the view of reaction kinetics [34].



$$\frac{dS_s}{dt} = -k_f S_s C_i^o + k_b S_{si} \quad (4)$$

Fig.5 is the experimental data shown as Fig. 2(a).

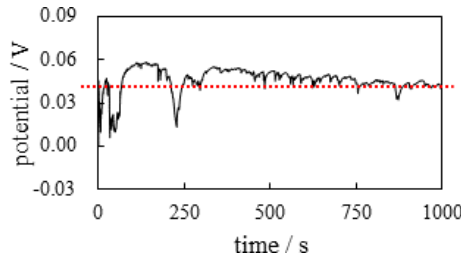


**Fig. 5:** Nickel wire surface potential vs. time The horizontal dotted line represents the hypothetical equilibrium potential.

We speculate that these potential spikes are caused by the repetitive adsorption-desorption process of  $i$  to  $s$  and such repetitive adsorption-desorption could be theorized in view of the stochastic process. Assuming that



8 *Spikes simulated by the SDE*

$C_i^o$  consists of the equilibrium constant part,  $\langle C_i \rangle_{eq}$ , and the Brownian motion part,  $\langle C_i \rangle_{Br}$ ,  $C_i^o$  is given by Eq. 5.

$$C_i^o = \langle C_i \rangle_{eq} + \langle C_i \rangle_{Br} \quad (5)$$

Given that  $\phi^o$  represents the equilibrium metal surface potential in reference to the potential at the bulk phase of KCl solution,  $\langle C_i \rangle_{eq}$  is given by Eq. 6 according to the Boltzmann distribution [32–37] where  $C_i^\infty$  and  $z_i$  represent the concentration of  $i$  at the bulk phase of KCl solution and the valency of  $i$ , respectively.  $\beta$  represents  $\frac{e}{2k_B T}$  ( $e$ : elementary charge,  $k_B$ : Boltzmann constant,  $T$ : solution temperature). We hypothesized that  $\langle C_i \rangle_{Br}$  obeys the normal distribution  $N(\mu, \sigma^2)$  ( $\mu$ : average,  $\sigma$ : standard deviation). We have to add a comment on  $\phi^o$ . The nickel wire surface potential always fluctuates. Therefore, an equilibrium surface potential does not exist when the nickel wire is used in reality. Therefore, in such a case,  $\phi^o$  is hypothetical but corresponds to the potential represented by the dotted line in Fig. 5

$$\langle C_i \rangle_{eq} \equiv C_i^\infty \exp(-2z_i \beta \phi^o) \quad (6)$$

Eq. 4 can be arranged into Eq. 7 using Eq. 5.

$$\begin{aligned} \frac{dS_s}{dt} &= -k_f S_s C_i^o + k_b S_{si} \\ &= -k_f S_s (\langle C_i \rangle_{eq} + \langle C_i \rangle_{Br}) + k_b (S_T - S_s) \\ &= -(k_f \langle C_i \rangle_{eq} + k_b) S_s - k_f S_s \langle C_i \rangle_{Br} + k_b S_T \end{aligned} \quad (7)$$

Since all the quantities,  $k_f$ ,  $k_b$ ,  $\langle C_i \rangle_{eq}$  and  $S_T$  are positive and constant, Eq. 7 can be arranged into Eq. 8 by employing  $P$ ,  $Q$ ,  $R$  and  $W$  defined by Eqs. 9a ~ 9c. Since  $dW$  is burdened with all the Brownian motion characteristics of  $\langle C_i \rangle_{Br} dt$ ,  $Q$  is inevitably considered as a negative constant quantity.

$$\begin{aligned} \frac{dS_s}{dt} &= -(k_f \langle C_i \rangle_{eq} + k_b)S_s - k_f S_s \langle C_i \rangle_{Br} + k_b S_T \\ \Leftrightarrow dS_s &= -(k_f \langle C_i \rangle_{eq} + k_b)S_s dt + QS_s dW + k_b S_T dt \\ \Leftrightarrow dS_s &= PS_s dt + QS_s dW + Rdt = (R + PS_s)dt + QS_s dW \end{aligned} \quad (8)$$

$$P \equiv -(k_f \langle C_i \rangle_{eq} + k_b) \quad (P < 0) \quad (9a)$$

$$QdW \equiv -k_f \langle C_i \rangle_{Br} dt \quad (Q < 0) \quad (9b)$$

$$R \equiv k_b S_T \quad (R > 0) \quad (9c)$$

Now, the calculation is performed using the Milstein scheme [38] where the time step is 0.001s. Figure 6 shows the  $S_s$  obtained by calculation. To obtain these diagrams, the numerical values of the parameters must be determined, but it is technically impossible to do this. Therefore, as a test, we have used Brownian motion obeying  $N(0, 3.0)$  (for Fig. 6 (a)) and  $N(0, 1.0)$  (for Fig. 6 (b)). But what numerical values are appropriate for the parameters  $P$ ,  $Q$  and  $R$ ? It is not permissible to choose the parameter values as one wishes, but the parameter values must be thermodynamically acceptable. As a test, we would like to use simple parameter values. For example, if Eq. 10 is established, Eq.

10 *Spikes simulated by the SDE*

11 could be achieved thermodynamically.

$$k_f \gg k_b \quad (10)$$

$$|P| \sim |Q| \quad (11)$$

Eqs. 9b and 9c suggest that Eq. 12 can be sufficed thermodynamically since Eq. 10 establishes and the relationship between  $\langle C_i \rangle_{eq}$  and  $\langle C_i \rangle_{Br}$  can determine the relationship between  $P$  and  $Q$ . Therefore, we consider the simplest parameter relationship given by Eq. 13 for the following computation.

$$|P| \sim |Q| \quad (12)$$

$$|P| \sim |Q| \sim |R| \quad (13)$$

We employed the parameters  $P$ ,  $Q$ , and  $R$  which are given by the constants -0.1, -0.1, and 0.05, respectively, for both Fig. 6(a) and (b). As stated at the end of the previous section “ $S_s$  (or  $S_T - S_{is}$ ) governs the metal surface potential characteristics,”  $S_s$  shown in Fig. 6 can qualitatively reflect the potential characteristics shown in Fig. 2. Quite intriguingly, Fig. 6 suggests that the standard deviation can rule the induction frequency of potential spike. We performed the same computation by choosing other  $\sigma$  numerical values and confirmed that the potential spike frequency increases by the increase of  $\sigma$ . Of course, there are many combinations of values for parameters ( $P$ ,  $Q$ ,

$R$ ,  $\mu$ ,  $\sigma$ ), we cannot derive the conclusion that the potential spike is in principle governed by the standard deviation  $\sigma$ . However, our stochastic model appears to be able to reproduce the high frequency of spike induction and the low frequency of spike induction as well. It is not against our intuition and it is not unthinkable that the surface properties of metal wire have significant influences on  $\sigma$ . Therefore, it is not inappropriate to say that  $\sigma$  is one of the governing parameters for the potential spike induction characteristics.

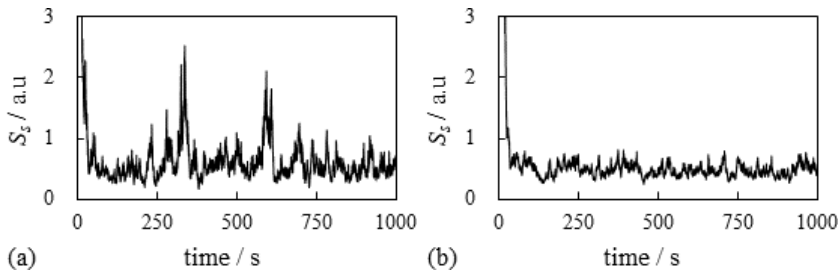


**Fig. 6:** Computationally calculated  $S_s$  vs. time (a)  $N(0, 3.0)$  (b)  $N(0, 1.0)$  Attention: The vertical axis does not represent the quantity of  $S_s$  but the ratio of  $S_s$ .

## 5 $S_s$ and potential

How is are the characteristics of  $S_s$  related to the potential behavior mathematically? Based on prior works described in the refs. [32, 33], the surface potential (we denote it here by  $\Phi$ ) and the surface charge (we denote it here by  $\Sigma$ ) can be mathematically associated with each other as given by Eq. 14 where  $\epsilon$ ,  $\epsilon_o$ ,  $U_o$ ,  $k_B$ , and  $T$  represent relative permittivity of water, vacuum permittivity, bulk phase ion concentration, Boltzmann constant, and the environmental temperature, respectively.

$$\Sigma = 2\sqrt{2\epsilon\epsilon_o U_o k_B T} \sinh(\beta\Phi) \quad (14)$$

12 *Spikes simulated by the SDE*

Eq. 14 can be arranged into Eq. 15.

$$\Phi = \frac{1}{\beta} \ln \left( \frac{\Sigma}{2\sqrt{2\epsilon\epsilon_o U_o k_B T}} + \sqrt{\left( \frac{\Sigma}{2\sqrt{2\epsilon\epsilon_o U_o k_B T}} \right)^2 + 1} \right) \quad (15)$$

Tamagawa and Ikeda previously studied the relationship between the surface potential of AgCl-coated Ag wire and its surface charge density when AgCl-coated Ag wire was submerged into the electrolytic solution, and they found that Eq. 16 was established [33]. Although the experimental conditions employed in their study were different from those employed in this study, we assume that Eq. 16 is applicable to this study, too, as a test. Therefore, Eq. 15 can be approximated into Eq. 17.

$$\left( \frac{\Sigma}{2\sqrt{2\epsilon\epsilon_o U_o k_B T}} \right)^2 \gg 1 \quad (16)$$

$$\Phi \sim \frac{1}{\beta} \ln \frac{\Sigma}{\sqrt{2\epsilon\epsilon_o U_o k_B T}} \quad (17)$$

$\Sigma$  is proportional to  $S_s$ . Hence,  $\Sigma$  can be expressed by Eq.18 by introducing a constant  $\kappa$ . Therefore, Eq. 17 can be further arranged into Eq. 19.

$$\Sigma = \kappa S_s \quad (18)$$

$$\Phi \sim \frac{1}{\beta} \ln \frac{\Sigma}{\sqrt{2\epsilon\epsilon_o U_o k_B T}} = \frac{1}{\beta} \ln \frac{\kappa_i S_s}{\sqrt{2\epsilon\epsilon_o U_o k_B T}} = \frac{1}{\beta} \ln S_s + const. \quad (19)$$

Setting  $const. = 0$  for Eq.19,  $\Phi$  was computed by plugging the numerical data of  $S_s$  of Fig. 6(a), and the outcome is shown in Fig. 7. So, the spike is generated and commented on Fig. 7. Although the experimental data shown in Fig. 5 shows that the potential spikes are all negative going, the computationally obtained spikes shown in Fig. 7 look positive going. It appears to be a serious mismatch between the experiment and the theory. However, the sign of potential is not an essential factor in this work at all. Whether the potential spikes are positive going or negative going depends merely on the sign of charges  $i$  bears and  $s$  bears. Once the sign of their charge becomes opposite, the sign of potential becomes opposite.

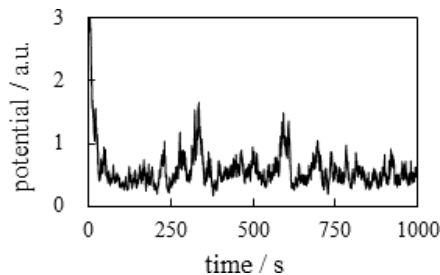


**Fig. 7:** Computationally obtained potential by converting the data of  $S_s$  in Fig. 6(a) Attention: The vertical axis does not represent the potential but the ratio of potential.

One may say that the potential profile shown in Fig. 7 exhibits too high a potential spike frequency compared with the actual experimental data in Fig. 2(a). But as stated earlier, we found that the potential spike frequency can change in accordance with the numerical value of  $\sigma$ . Our emphasis here does not lie in that our theoretical model can quantitatively reproduce the

experimental potential profiles but in that the potential characteristics could be stochastically determined. Figure 8 shows the potential profiles of the time  $t = 100\text{s} \sim 250\text{s}$  (time range was chosen unintentionally) when  $N(\mu, \sigma) = N(0, 3.0)$ ,  $N(0, 1.0)$  and  $N(0, 0.5)$ , is a clear example that the frequency of the articulate potential spikes increases with the increase of  $\sigma$ , though all the profiles exhibit the small fluctuation continuously (No fluctuation cannot take place in nature).

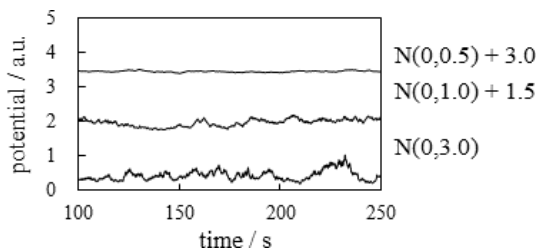


**Fig. 8:** Computationally obtained potential profiles for (a)  $N(0, 3.0)$  (b)  $N(0, 1.0)$  (c)  $N(0, 0.5)$ . The profiles for  $N(0, 1.0)$  and  $N(0, 0.5)$  are shifted upward by  $+1.5$  and  $+3.0$ , respectively, so that the profiles overlap one another.

Furthermore, we even observed that the high frequency of potential spike can be experimentally achieved by employing a different experimental condition than the condition employed for obtaining the experimental potential shown in Fig. 2(a). Fig. 9 shows the potential profile of nickel wire submerged in a 1M NaCl solution. It exhibited a higher potential spike frequency compared with the potential profile shown in Fig. 2(a). In other words, the potential characteristics predicted by our theoretical model exist in the actual experimental system.

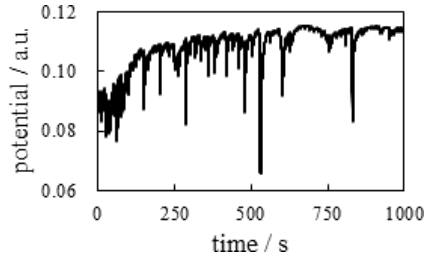


**Fig. 9:** Experimentally measured surface potential of nickel wire submerged in a 1M NaCl solution.

The spike generation mechanism could be explained by the inanimate model based on the stochastic process. The induction of potential spikes in the living system could also be explained by this type of inanimate stochastic model. No life activity is required even for the induction of the cell's potential peak. Although the computationally obtained potential profiles are not quantitatively the same as the real experimental potential profiles, the qualitative aspects are similar to each other. Therefore, we cannot exclude the ion adsorption-desorption mechanism as a mechanism for the generation of the action potential.

## 6 Conclusion

The inanimate experimental system showed potential spikes and the stochastic model reproduced the induction of potential spikes. The laws of physics never distinguish between living and non-living systems. Therefore, it is not abnormal to think that the potential spikes of a living cell can also be explained by the stochastic model. Stochastic processing of neuron activity is not a new work, but such a mathematical tool has been used in the study of neuroscience [39–41] although it is not so popular. However, our way of incorporating the stochastic process into neurodynamic analysis is quite distinct from others, such as conventional work. Conventional work is a combination of ordinal



neurodynamic theory and the stochastic process. On the other hand, the repetitive occurrence of the ion adsorption-desorption process is responsible for the generation of potential peaks in our model, and we have incorporated the stochastic process into the kinetics of the ion adsorption-desorption reaction. Our result explains relatively well the characteristics of the generation of the cellular action potential. From our stochastic model for neurodynamics, we believe that the inanimate model should not be excluded as a mechanism for action potential generation.

**Declaration of COI:** All the authors state that there is no conflict of interests.

## References

- [1] J. Cronin, *Mathematical Aspects of Hodgkin-Huxley Neural Theory*, Cambridge University Press, New York, 1987.
- [2] G. B. Ermentrout and D. H. Terman, *Mathematical Foundations of Neuroscience (Interdisciplinary Applied Mathematics Book 35)*, Springer, New York, 2010.
- [3] J. Keener and J. Sneyd, *Mathematical Physiology: I: Cellular Physiology (Interdisciplinary Applied Mathematics)*, Springer, New York, 2008.
- [4] G. N. Ling, *A Revolution in the Physiology of the Living Cell*, Krieger Pub Co, Malabar, Florida, 1992.
- [5] G. N. Ling, *Life at the Cell and Below-Cell Level: The Hidden History of a Fundamental Revolution in Biology*, Pacific Press, New York, 2001.

- [6] G. N. Ling, Debunking the alleged resurrection of the sodium pump hypothesis, *Physiol. Chem. Phys.*, 29 (1997) 123–198.
- [7] Y. ISHIMA, A. T. PRZYBYLSKI and S. W. FOX, ELECTRICAL MEMBRANE PHENOMENA IN SPHERULES FROM PROTEINOID AND LECITHIN, *BioSystems*, 69 (1981) 243–251.
- [8] A. T. Przybylski, W. P. Stratten, R. M. Syren and S. W. Fox, Membrane, Action, and Oscillatory Potentials in Simulated Protocells, *Die Naturwissenschaften*, 69 (1982) 561–563.
- [9] A. T. Przybylski and S. W. Fox, Excitable Artificial Cells of Proteinoid, *Physiol. Applied Biochemistry and Biotechnology*, 10 (1984) 301–307.
- [10] K. MATSUNO, ELECTRICAL EXCITABILITY OF PROTEINOID MICROSPHERES COMPOSED OF BASIC AND ACIDIC PROTEINOIDS, *BioSystems*, 17 (1984) 11–14.
- [11] A. T. Przybylski and S. W. Fox, EXCITABLE CELL MADE OF THERMAL PROTEINOIDS, *BioSystems*, 17 (1985) 281–288.
- [12] G. VAUGHAN, A. T. PRZYBYLSKI and S. W. FOX, THERMAL PROTEINOIDS AS EXCITABILITY-INDUCING MATERIALS, *BioSystems*, 20 (1987) 219–223.
- [13] K. Haefner, (Ed), *Evolution of Information Processing Systems An Interdisciplinary Approach for a New Understanding of Nature and Society*, Springer, New Yorka, 1992.
- [14] S. W. Fox, P. R. Bahn, K. Dose, K. Harada, L. Hsu, Y. Ishima, J. Jungck, J. Kendrick, G. Krampitz, J. C. Lacey, Jr., K. Matstmo, P.

- Melius, M. Middlebrook, T. Nakashima, A. Pappelis, A. Pol, d. l. Rohlfing, a. Vegotsky, T. v. Waelmeltdt, H. Wax and B. Yu, EXPERIMENTAL RETRACEMENT OF THE ORIGINS OF A PROTOCELL: *It Was Also A Protoneuron*, 20 (1994) 17–36.
- [15] K. YOSHIKAWA and Y. MATSUBARA, SPONTANEOUS OSCILLATION OF ELECTRICAL POTENTIAL ACROSS ORGANIC LIQUID MEMBRANES, *Biophysical Chemistry*, 17 (1983) 183–185.
- [16] K. YOSHIKAWA, K. SAKABE, Y. MATSUBARA and T. OTA, OSCILLATION OF ELECTRICAL POTENTIAL IN A POROUS MEMBRANE DOPED WITH GLYCEROL  $\alpha$ -MONOOLEATE INDUCED BY AN  $\text{Na}^+/\text{K}^+$  CONCENTRATION GRADIENT, *Biophysical Chemistry*, 20 (1984) 107–109.
- [17] K. YOSHIKAWA, K. SAKABE, Y. MATSUBARA and T. OTA, SELF-EXCITATION IN A POROUS MEMBRANE DOPED WITH SORBITAN MONOOLEATE (SPAN-80) INDUCED BY AN  $\text{Na}^+/\text{K}^+$  CONCENTRATION GRADIENT, *Biophysical Chemistry*, 21 (1985) 33–39.
- [18] K. TOKO, K. YOSHIKAWA, M. TSUKIJI, M. NOSAKA and K. YAMAFUJI, N THE OSCILLATORY PHENOMENON IN AN OIL/WATER INTERFACE, *Biophysical Chemistry*, 22 (1985) 151–158.
- [19] K. YOSHIKAWA, T. OMOCHI and Y. MATSUBARA, CHEMORECEPTION OF SUGARS BY AN EXCITABLE LIQUID MEMBRANE, *Biophysical Chemistry*, 23 (1986) 211–214.
- [20] K. YOSHIKAWA, T. OMOCHI, Y. MATSUBARA and H. KOURAI, A POSSIBILITY TO RECOGNIZE CHIRALITY BY AN EXCITABLE

- ARTIFICIAL LIQUID MEMBRANE, *Biophysical Chemistry*, 24 (1986) 111–119.
- [21] K. Yoshikawa, M. Shoji, S. Nakata and S. Maeda, An Excitable Liquid Membrane Possibly Mimicking the Sensing Mechanism of Taste, *Langmuir*, 4 (1988) 759–762.
- [22] N. NAKAJO, K. YOSHIKAWA, M. SHOJI and I. UEDA, SPONTANEOUS OSCILLATION OF ARTIFICIAL MEMBRANE: EQUIVALENCE IN EFFECTS OF TEMPERATURE AND VOLATILE ANESTHETIC, *BIOCHEMICAL AND BIOPHYSICAL RESEARCH COMMUNICATIONS*, 167 (1990) 450–456.
- [23] M. Saito, T. Koyano, Y. Miyamoto, K. Kaifu, M. Kato and K. Kawamura, Electric Self-sustained Oscillations of a DOPH-Millipore Membrane induced by Acid, *MEMBRANE*, 15 (1990) 228–230.
- [24] J. Srividhya and M. S. Gopinathan, Modeling Experimental Oscillations in Liquid Membranes with Delay Equations, *J. Phys. Chem. B*, 107 (2003) 1438–1443.
- [25] J. Gao, L. Wang, W. Yang and F. Yang, Electrical Potential Oscillation in an Anionic Surfactant System with Barbitone in Octanol as an Oil Phase, *Journal of the Iranian Chemical Society*, 2 (2005) 71–77.
- [26] T. Ogawa, H. Shimazaki, S. Aoyagi and S. Sakai, Novel modeling of electrical potential oscillation across a water/octanol/water liquid membrane, *Journal of Membrane Science*, 285 (2006) 120–125.
- [27] J. Z. Gao, H. X. Dai, H. Chen, J. Ren and W. Yang, Study on the oscillating phenomena of electrical potential across a liquid membrane, *Chinese*

20 *Spikes simulated by the SDE*

Chemical Letters, 18 (2007) 309–312.

- [28] N. M. Kovalchuk, Spontaneous non-linear oscillations of interfacial tension at oil/water interface, *Open Chem.*, 13 (2015) 1–16.
- [29] Y. Li, M. B. Ives and K. S. Coley, Corrosion potential oscillation of stainless steel in concentrated sulphuric acid: I. Electrochemical aspects, *Corrosion Science*, 48 (2006) 1560–1570.
- [30] S. Jones, Y. Li, K. S. Coley, J. R. Kish and M. B. Ives, Corrosion potential oscillations of nickel-containing stainless steel in concentrated sulphuric acid: II Mechanism and kinetic modelling, *Corrosion Science*, 52 (2010) 250–254.
- [31] D. Sazou, M. Pavlidou and M. Pagitsas, Potential oscillations induced by localized corrosion of the passivity on iron in halide-containing sulfuric acid media as a probe for a comparative study of the halide effect, *Corrosion Science*, 675 (2012) 54–67.
- [32] H. Tamagawa, Mathematical expression of membrane potential based on Ling’s adsorption theory is approximately the same as the Goldman-Hodgkin-Katz equation, *J. Biol. Phys.*, 45 (2018) 13–30.
- [33] H. Tamagawa and K. Ikeda, Another interpretation of Goldman-Hodgkin-Katz equation based on the Ling’s adsorption theory, *Eur. Biophys. J.*, 47 (2018) 869–879.
- [34] G. M. Barrow, *Physical Chemistry*, McGraw-Hill Inc., New York, 1984.
- [35] A. Kitahara and A. Watanabe, *Surfactant Science Series Volume 15, Electrical Phenomena at Interface Fundamentals, Measurements, and*

- Applications, Dekker, New York, 1984.
- [36] J. O'M. Bockris, *Surface Electrochemistry: A Molecular Level Approach*, Springer, New York, 1993.
- [37] C. M. A. Brett and A. M. O. Brett, *Electrochemistry Principles, Methods and Applications*, Oxford University Press, New York, 1993.
- [38] Peter E. Kloeden and Eckhard Platen, *Numerical solution of stochastic differential equations*, Springer, New York, 1992.
- [39] P. Holmes, E. Brown, J. Moehlis, R. Bogacz, J. Gao, P. Hu, G. Aston-Jones, E. Clayton, J. Rajkowski and J.D. Cohen, *Optimal decisions: From neural spikes, through stochastic differential equations, to behavior*, 2004 International Symposium on Nonlinear Theory and its Applications (NOLTA2004), Fukuoka, Japan, Nov. 29 - Dec. 3, 2004.
- [40] J. H. Goldwyn, N. S. Imenov, M. Famulare and E. Shea-Brown, *Stochastic differential equation models for ion channel noise in Hodgkin-Huxley neurons*, 83 (2011) 041908.
- [41] P. F. Rowat and P. E. Greenwood, *The ISI distribution of the stochastic Hodgkin-Huxley neuron*, *Front. Comput. Neurosci.*, 8 (2014) 1–12.